Report Documentation Page

Form Approved
OMB No. 0704-0188

1. REPORT DATE	2. REPORT TYPE	3. DATES COVERED
AUG 2000		**00-00-2000 to 00-00-2000**

4. TITLE AND SUBTITLE	5a. CONTRACT NUMBER
Proton irradiation of InAs/AlSb/GaSb resonant interband tunneling diodes	5b. GRANT NUMBER
	5c. PROGRAM ELEMENT NUMBER
6. AUTHOR(S)	5d. PROJECT NUMBER
	5e. TASK NUMBER
	5f. WORK UNIT NUMBER
7. PERFORMING ORGANIZATION NAME(S) AND ADDRESS(ES) **Naval Research Laboratory,4555 Overlook Avenue SW,Washington,DC,20375**	8. PERFORMING ORGANIZATION REPORT NUMBER
9. SPONSORING/MONITORING AGENCY NAME(S) AND ADDRESS(ES)	10. SPONSOR/MONITOR'S ACRONYM(S)
	11. SPONSOR/MONITOR'S REPORT NUMBER(S)

12. DISTRIBUTION/AVAILABILITY STATEMENT
Approved for public release; distribution unlimited

13. SUPPLEMENTARY NOTES

14. ABSTRACT

15. SUBJECT TERMS

16. SECURITY CLASSIFICATION OF:			17. LIMITATION OF ABSTRACT	18. NUMBER OF PAGES	19a. NAME OF RESPONSIBLE PERSON
a. REPORT	b. ABSTRACT	c. THIS PAGE			
unclassified	**unclassified**	**unclassified**	**Same as Report (SAR)**	**3**	

Proton irradiation of InAs/AlSb/GaSb resonant interband tunneling diodes

R. Magno,[a] B. D. Weaver, A. S. Bracker, and B. R. Bennett
Naval Research Laboratory, Washington, DC 20375-5347

(Received 3 August 2000; accepted for publication 14 February 2001)

Room temperature current–voltage measurements have been made on InAs/AlSb/GaSb resonant interband tunnel diodes irradiated with 2 MeV protons to determine the effect of displacement damage on the negative resistance peak current I_p and the peak-to-valley current ratio P/V. Diodes with 5 and 13 ML AlSb barrier thickness were irradiated and measured several times until the total fluences reached 1×10^{15} and $2\times10^{14}\,H^+/cm^2$, respectively. The current due to radiation-induced defects has a nonlinear voltage dependence, with a large increase occurring in the voltage range between the negative resistance peak and the valley. I_p increased $<50\%$ while a large increase in the valley current decreased the P/V ratios to about 2. [DOI: 10.1063/1.1363697]

Resonant interband tunneling diodes (RITDs) composed of InAs/AlSb/GaSb/AlSb/InAs heterostructures[1] are of interest for applications in highly functional, low-power logic circuits at frequencies approaching 100 GHz.[2] These applications require diodes with a large peak-to-valley current ratio (P/V), and a peak current density in the range of $1\times10^5\,A/cm^2$. Because the negative resistance peak occurs near 100 meV in this material system, it may be possible to produce logic circuits with lower power consumption than those made with other material systems.[3] Interband tunneling involves the transport of an electron from the conduction band of one InAs electrode to another through the valence band of a GaSb well sandwiched between AlSb barriers. A detailed calculation of the tunneling current for these interband tunneling diodes remains to be done, but in its simplest form it will invoke the concepts of energy conservation and conservation of momentum parallel to the interface. A more complete analysis may need to include scattering phenomena involving phonons, impurities, and interfaces. The charge trapped on impurities or stoichiometric defects such as antisites, interstitials, and vacancies will also contribute to the static potential that determines the overlap of the InAs electrode energy bands with the GaSb quantum-well subbands. The proton irradiations used here are a convenient way of introducing displacement damage such as vacancies, interstitials, and antisites. Observing the response to the irradiation is a path to determining the influence of growth-induced stoichiometric defects on the size of the peak and valley currents.[4] In addition, these measurements will provide information on the radiation hardness of RITDs to aid in determining whether these devices may be useful in satellite systems where power consumption and weight are important considerations.

The samples examined here were grown by molecular-beam epitaxy on semi-insulating GaAs substrates. To accommodate for the 8% lattice mismatch between the GaAs and AlSb/GaSb/AlSb quantum-well structure, a buffer layer consisting of 0.15 μm of AlSb followed by 1 μm of $n^+(3\times10^{18}\,Si\,cm^{-3})$ was grown first. The RITD structure consists of a pair of nominally identical AlSb barriers sandwiching a 27 ML GaSb well. The InAs 40 ML (12 nm) layers adjacent to both AlSb barriers were undoped, and the next 30 nm InAs layers away from the barriers were doped with $1\times10^{17}\,Si\,cm^{-3}$. Finally, a 200 nm layer of $3\times10^{18}\,Si\,cm^{-3}$ InAs was grown on top of the RITD. Growth procedures were used to form InSb interface bonds at the InAs/AlSb interfaces.[5] Reflection high-energy electron diffraction measurements were used to calibrate growth rates in order to determine the thicknesses of the RITD layers. Sample temperatures during growth were 440 °C. The temperature was monitored by a thermocouple, calibrated to the congruent sublimation temperature of InAs, ~460 °C. Standard photolithography techniques were used to pattern Ti/Pt/Au Ohmic contacts with diameters ranging from 2 to 50 μm. Mesas were formed by using the Ohmic contacts as the etch stop in a wet-etching process. Current–voltage ($I-V$) measurements were made at room temperature by tensioning a fine gold wire point contact against the Ohmic contact. (In the data plots, ''positive bias'' means the top of the mesa is biased positively with respect to the substrate.) To determine if the response depends on barrier thickness two nominally identical samples, one with 13 ML and the other with 5 ML barriers, were irradiated.

Irradiations were performed using 2 MeV protons incident at 7° to the surface normal in order to discourage ion channeling effects. Protons of this energy create mostly point defects, such as vacancies, interstitials, and Frenkel pairs. The average range of 2 MeV protons is approximately 30 μm, which means that the protons stopped far below the AlSb/GaSb/AlSb layers in the GaAs substrate. The RITDs were irradiated incrementally up to maximum fluences of 2×10^{14} and $1\times10^{15}\,H^+/cm^2$ for the 13 and 5 ML (i.e., low- and high-current) devices, respectively. Calculations using the Monte Carlo program SRIM (Ref. 6) show that the initial concentration of defects at the maximum fluences is about 6×10^{-5} and 9×10^{-4} displacements per target-material atom (dpa) for the low- and high-current devices. Recombination events between interstitials and vacancies along the proton track may reduce the initial defect concentrations, resulting in a lower defect concentration.

$I-V$ measurements were made on nine individual diodes for each sample following an irradiation. The irradiation/

[a]Electronic mail: magno@bloch.nrl.navy.mil

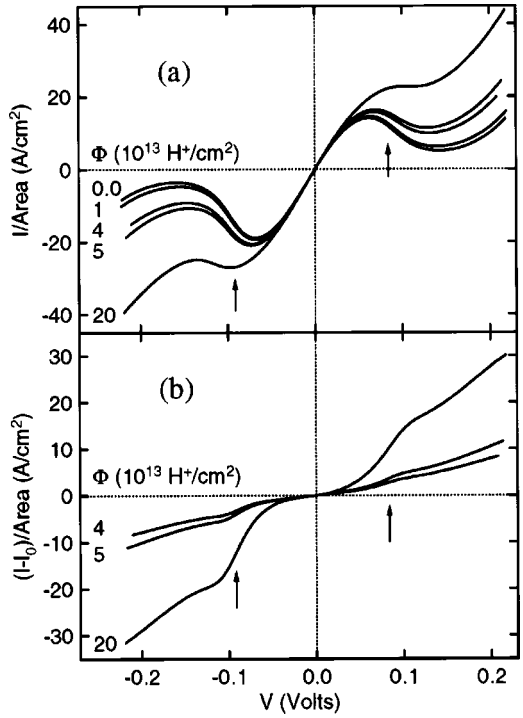

FIG. 1. (a) $I-V$ data before and after several irradiations of a diode with 13 ML AlSb barriers. (b) Differences found by subtracting I_0, the $I-V$ for the unirradiated diode, from the $I-V$ for $\Phi=2\times10^{14}$, 5×10^{13}, and 4×10^{13} H^+/cm^2.

measurement cycle was repeated until the P/V ratio deteriorated to approximately 1 for the low current device and 2 for the high current one. For mesas with diameters larger than 15 μm, the same mesa was measured after each irradiation, but for the smaller diameter devices, it was impossible to contact the same device for each measurement.

$I-V$ data for a 20-μm-diam diode with 13-ML-thick barriers before irradiation and after irradiation with several fluences, Φ, are illustrated in Fig. 1(a). The primary effects of proton irradiation are a large increase in the valley current and a smaller increase in the peak current. Similar measurements were made on a sample with 5 ML AlSb barriers that prior to irradiation had a peak current density of 1.2×10^4 A/cm^2, and a P/V ratio of 15. With subsequent irradiations, both samples exhibited a slight increase in the peak current while the valley current increased rapidly.

Summaries of the fluence dependence of the peak and valley currents for both bias polarities for both samples are presented in Figs. 2(a) and 2(b). The data points in Fig. 2 are average values of the peak and valley currents measured for the nine diodes for each sample. The peak and valley currents are displayed for both bias polarities, in order to demonstrate that there is no obvious asymmetry in the damage. The relative sensitivity of the two devices to the irradiation may be found by comparing the data in Fig. 2. The data indicate that the first noticeable change in the valley current for the high current diode, Fig. 2(a), is at 4×10^{13} H^+/cm^2, while in Fig. 2(b) the first change for the low-current one is at $\Phi=1\times10^{13}$ H^+/cm^2. The P/V ratio for the low-current device deteriorated to near unity at a fluence of 2×10^{14} H^+/cm^2, while $P/V\cong2$ is found for the high-current sample at a fluence of 1×10^{15} H^+/cm^2. These observations indicate the low-current diodes are more susceptible to radiation-induced damage than the high-current ones.

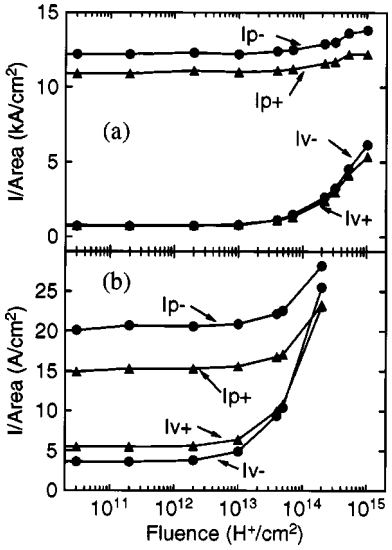

FIG. 2. Fluence dependence for the positive and negative bias peak currents, Ip_+, Ip_-, and the valley currents Iv_+, Iv_- for (a) 5 ML and (b) 13 ML AlSb barrier samples.

Another comparison of the relative sensitivity of the two samples to radiation damage is made by subtracting the peak current prior to irradiation from the peak current after irradiation and normalizing the difference by the fluence. A similar normalized difference for the valley currents has also been calculated. These differences can be interpreted as the excess current per proton, and are plotted in Figs. 3(a) and 3(b) for the high- and low-current diodes, respectively, for fluences above 1×10^{13} H^+/cm^2 where the largest current increases take place. While the fluence-normalized incremental valley currents vary somewhat with fluence, a rough comparison may be made by taking 9 pA/H^+ as the average value for the 5 ML barrier and 0.12 pA/H^+ for the 13 ML one. The ratio of these averages indicates that about 75 times more excess current per proton flows through the sample with the thinner AlSb barriers than the one with the thicker barriers. While this number makes the thinner barrier device

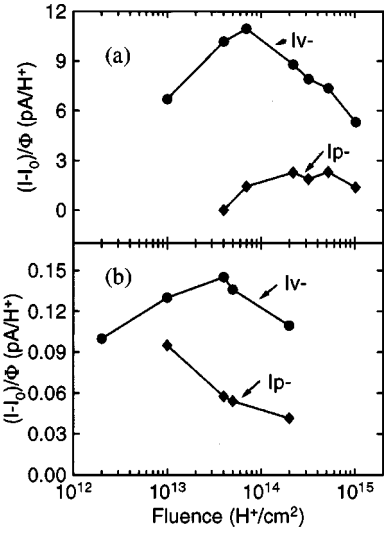

FIG. 3. Difference between the peak currents before and after irradiation and valley currents before and after irradiation normalized by fluence Φ for the samples with (a) 5 ML and (b) 13 ML AlSb barriers.

look more sensitive to the proton irradiation, it is important to remember that the ratio of the unirradiated peak currents is 600 to 1, so a larger fluence is necessary to reduce the higher current device to the same P/V as the lower current one. The difference in the incremental current per proton should aid in understanding how radiation-induced defects influence the current through these devices.

The bias dependence of the current added by the irradiation-induced defects also adds information about the defect-assisted current flow. This is illustrated in Fig. 1(b) for the low-current sample by plotting the differences between the $I-V$ curves for three highest fluences and the $I-V$ data, I_0, prior to irradiation. The added current increases in a nonlinear fashion with a significant increase found in the voltage range between the peak and the valley currents. The voltages where the defect-assisted currents increase fastest are indicated by the arrows in Figs. 1(a) and 1(b). These points were found by numerically differentiating the difference curves. It is interesting that the defect-assisted current increases with bias more rapidly in a range where the tunneling current is being cut off.

The results obtained here may be compared with those found for resonant tunneling diodes (RTDs), where the tunneling occurs via conduction bands in the emitter, collector, and well. Only one barrier thickness was used for the study of proton irradiation effects in an InP-based RTD with InGaAs electrodes, AlAs barriers, and an InGaAs/InAs/InGaAs well.[7–9] This RTD is more sensitive to proton irradiation than the 5 ML AlSb barrier RITD reported here, but less so than the 13 ML AlSb one. A significant difference between the two types of devices is that the RTD peak current decreases with fluence while the RITD peak current increases. The valley current increases with increasing fluence for both the RTD and RITDs, though they have different dependences on voltage. The fluence-normalized difference curves for the RTDs overlap giving a universal curve that is proportional to V^3 in the regions away from the resonance. When normalized by the fluence, the difference curves in Fig. 1(b) do not fall on a universal curve, and their bias dependence is not proportional to V^3.

The current flow in RITDs is significantly different from that in RTDs because the band offsets result in transport via valence bands in the RITD well rather than by conduction-band states as in the well of a RTD. Also, as a result of the band offsets, a negative resistance with a P/V less than 2 is found in the RITD even if there are no AlSb barriers.[10] A possible defect-induced current mode for the RITDs is that when a proton creates a primary knock-on displacement, the knock-on can in turn cause a short, but dense, oblong terminal cluster (or ''trail'') of secondary displacements. If this trail passes through an AlSb barrier, it may result in a small conducting filament carrying a leakage current having a nonlinear bias dependence. The filament may not penetrate entirely through a 13 ML barrier, resulting in a smaller current per proton compared to a similar trail passing through a 5 ML barrier. While the damage-induced current per proton is smaller for the 13 ML RITD than for the 5 ML one, fewer protons are required to reduce the P/V as the peak and valley currents prior to irradiation are much smaller than those of the 5 ML RITD.

In summary, the sensitivity of InAs/AlSb/GaSb RITDs to 2 MeV proton irradiation has been examined. Diodes with 13 ML AlSb barriers are more sensitive than ones with 5 ML barriers. Both the peak and valley currents increased with increasing fluence, but the increase in the valley current was faster than the peak current. A possible explanation is that through secondary displacements protons create conducting leakage paths in the AlSb barriers.

This research was supported in part by the Office of Naval Research.

[1] J. R. Söderström, D. H. Chow, and T. C. McGill, Appl. Phys. Lett. **55**, 1094 (1989).
[2] B. R. Bennett, A. S. Bracker, R. Magno, J. B. Boos, R. Bass, and D. Park, J. Vac. Sci. Technol. B **18**, 1650 (2000).
[3] K. J. Chen, K. Maezawa, and M. Yamamoto, IEEE Electron Device Lett. **17**, 127 (1996).
[4] K. Shiralagi, J. Shen, and R. Tsui, J. Electron. Mater. **26**, 1417 (1997).
[5] B. Z. Nosho, W. H. Weinberg, W. Barvosa-Carter, A. S. Bracker, R. Magno, B. R. Bennett, J. C. Culbertson, B. V. Shanabrook, and L. J. Whitman, J. Vac. Sci. Technol. B **17**, 1786 (1999).
[6] J. F. Ziegler, J. P. Biersack, and U. Littmark, *The Stopping and Range of Ions in Solids* (Pergamon, New York, 1985), Vol. 1; the latest version of SRIM is available online at http://www.research.ibm.com/ionbeams.
[7] E. M. Jackson, B. D. Weaver, A. C. Seabaugh, J. P. A. Van der Wagt, and E. A. Beam III, Appl. Phys. Lett. **75**, 280 (1999).
[8] B. D. Weaver, E. M. Jackson, A. C. Seabaugh, and J. P. Van der Wagt, Appl. Phys. Lett. **76**, 2562 (2000).
[9] B. D. Weaver, E. M. Jackson, G. P. Summers, and A. C. Seabaugh, J. Appl. Phys. **88**, 6951 (2000).
[10] D. A. Collins, E. T. Yu, Y. Rajakarunanayake, J. R. Söderström, D. Z.-Y. Ting, D. H. Chow, and T. C. McGill, Appl. Phys. Lett. **57**, 683 (1990).